

RESEARCH ARTICLE

Cancer- and behavior-related genes are targeted by selection in the Tasmanian devil (*Sarcophilus harrisii*)

Jean-Noël Hubert*, Tatiana Zerjal, Frédéric Hospital

GABI, INRA, AgroParisTech, Université Paris-Saclay, Jouy-en-Josas, France

* jean-noel.hubert@inra.fr



Abstract

Devil Facial Tumor Disease (DFTD) is an aggressive cancer notorious for its rare etiology and its impact on Tasmanian devil populations. Two regions underlying an evolutionary response to this cancer were recently identified using genomic time-series pre- and post-DFTD arrival. Here, we support that DFTD shaped the genome of the Tasmanian devil in an even more extensive way than previously reported. We detected 97 signatures of selection, including 148 protein coding genes having a human orthologue, linked to DFTD. Most candidate genes are associated with cancer progression, and an important subset of candidate genes has additional influence on social behavior. This confirms the influence of cancer on the ecology and evolution of the Tasmanian devil. Our work also demonstrates the possibility to detect highly polygenic footprints of short-term selection in very small populations.

OPEN ACCESS

Citation: Hubert J-N, Zerjal T, Hospital F (2018) Cancer- and behavior-related genes are targeted by selection in the Tasmanian devil (*Sarcophilus harrisii*). PLoS ONE 13(8): e0201838. <https://doi.org/10.1371/journal.pone.0201838>

Editor: Mathew S. Crowther, University of Sydney, AUSTRALIA

Received: February 27, 2018

Accepted: July 22, 2018

Published: August 13, 2018

Copyright: © 2018 Hubert et al. This is an open access article distributed under the terms of the [Creative Commons Attribution License](https://creativecommons.org/licenses/by/4.0/), which permits unrestricted use, distribution, and reproduction in any medium, provided the original author and source are credited.

Data Availability Statement: Data are from the Epstein et al. (2016) study and can be accessed on Dryad (<https://doi.org/10.5061/dryad.r60sv>).

Funding: JNH was supported by the French Ministry of Higher Education and Research. The funder had no role in study design, data collection and analysis, decision to publish, or preparation of the manuscript.

Competing interests: The authors have declared that no competing interests exist.

Introduction

Understanding the role of selection in the resistance against cancer should benefit from the study of animal populations. Domestic populations that develop spontaneous neoplasms similar to those encountered in humans have been increasingly investigated to unravel the complex genetic determinism of some cancers [1]. Studies that examine cancer in natural populations are, however, quite rare, despite their potential for improving our knowledge of cancer resistance mechanisms in an ecological context. Observations made in this field are limited to a small number of unique cancer evolution cases, as those described in the naked-mole rat, the elephant, and the Tasmanian devil [2]. In particular, horizontally transmitted cancers remain rarely observed events in nature, and so far they have been described in dogs [3], the Tasmanian devil [4] and several species of bivalves [5]. A well-known case of transmissible cancer is the one affecting the Tasmanian devil (*Sarcophilus harrisii*), the largest existing marsupial carnivore. This cancer, known as the Devil Facial Tumor Disease (DFTD), is characterized by a recent emergence, a high propensity to metastasize, and a mortality rate close to 100% within 12 months after infection [6,7,8,9]. The disease was first detected in north-eastern Tasmania in 1996 and has since spread across 95% of the species' range [10] through biting injuries during social contact [11]. DFTD has induced a rapid decline and a very strong selective pressure on the Tasmanian devil—with local population losses over 90%—giving rise to serious concerns regarding the species survival on the short term [12].

DFTD has become a very well documented case study over the past decade. This amount of data is a valuable resource to better understand cancer biology and is expected to provide insight into the mechanisms underlying immunosurveillance of cancer initiation and metastatic spreading [7]. A recent analysis of Tasmanian devil genomic time-series [13] led to the identification of two regions exhibiting signatures of selection in response to DFTD which contain genes related to cancer risk and immune function in humans [14]. Here, we extend this research by using a customized maximum-likelihood method that has been shown efficient for investigating rapid selection in experimental populations when genomic time-series data are available [15]. In comparison to the approach used in [14], our method has in particular the advantage of efficiently disentangling the effects of strong selection from those of strong drift in a population-specific manner. In total, 97 genomic regions harboring 148 protein coding genes with human orthologues were identified. The functional analysis revealed that all the functionally characterized orthologues have a link with cancer and around 15% are involved in the functioning of the Central Nervous System (CNS), with about fifteen genes associated with behavioral disorders.

Our data support the view that the evolutionary response to DFTD consists in several strategies that rely on a larger range of genetic variants than previously thought. These findings should contribute to a better understanding of the ecology and evolution of both the Tasmanian devil and cancer. In particular, this should help to pinpoint some genes that may provide host populations with a “resistance”—either by improving cancer survival or by reducing the risk of infection—to a transmissible cancer.

Results

Signatures of selection in the Tasmanian devil genome

Our analysis resulted in the identification of 97 signatures of selection dispersed throughout the chromosomes, accounting for about 0.3% of the genome. Most signatures of selection were found to be population-specific, and only one was common to the three investigated populations (Fig 1A). The West Pencil Pine (WP), Freycinet (FN) and Narawntapu (NP) populations displayed 54, 38 and 37 signatures of selection, respectively (Fig 1B). The ability to detect signatures of selection from the dataset was influenced by the experimental sampling protocol and SNP detection, which was specific to each population (Table 1). In the WP population, characterized by an adequate time-series sampling but with a low SNP density, a large number of small signatures of selection were detected. In the NP population, despite a high SNP density, a low proportion of candidate SNP (0.4%) was detected. This can be explained by the non-optimal sampling time-series (Table 1), with the latest data point too close to the date of arrival of the disease, which left little time for selection to produce visible effects. The FN population presented a much better SNP density and sampling time-series, compared to the other populations, which allowed detecting the highest number of candidate SNP (210) and larger signatures of selection. As a consequence, a larger proportion (68%) of candidate regions were located less than 100 kb from a protein coding gene in the FN population (Fig 1B). In total, for the three populations, 60 signatures of selection were detected in the vicinity of protein coding genes with a human orthologue (see S1 Fig and S1 Table for the details) allowing us to identify 148 candidate genes according to Ensembl genome browser 90 (S1 Table).

The functional annotation of candidate genes reveals a strong link with cancer

We used the IPA knowledge base analysis tool (Ingenuity Systems®, www.ingenuity.com) to identify biological functions and disease-related categories associated with our candidate

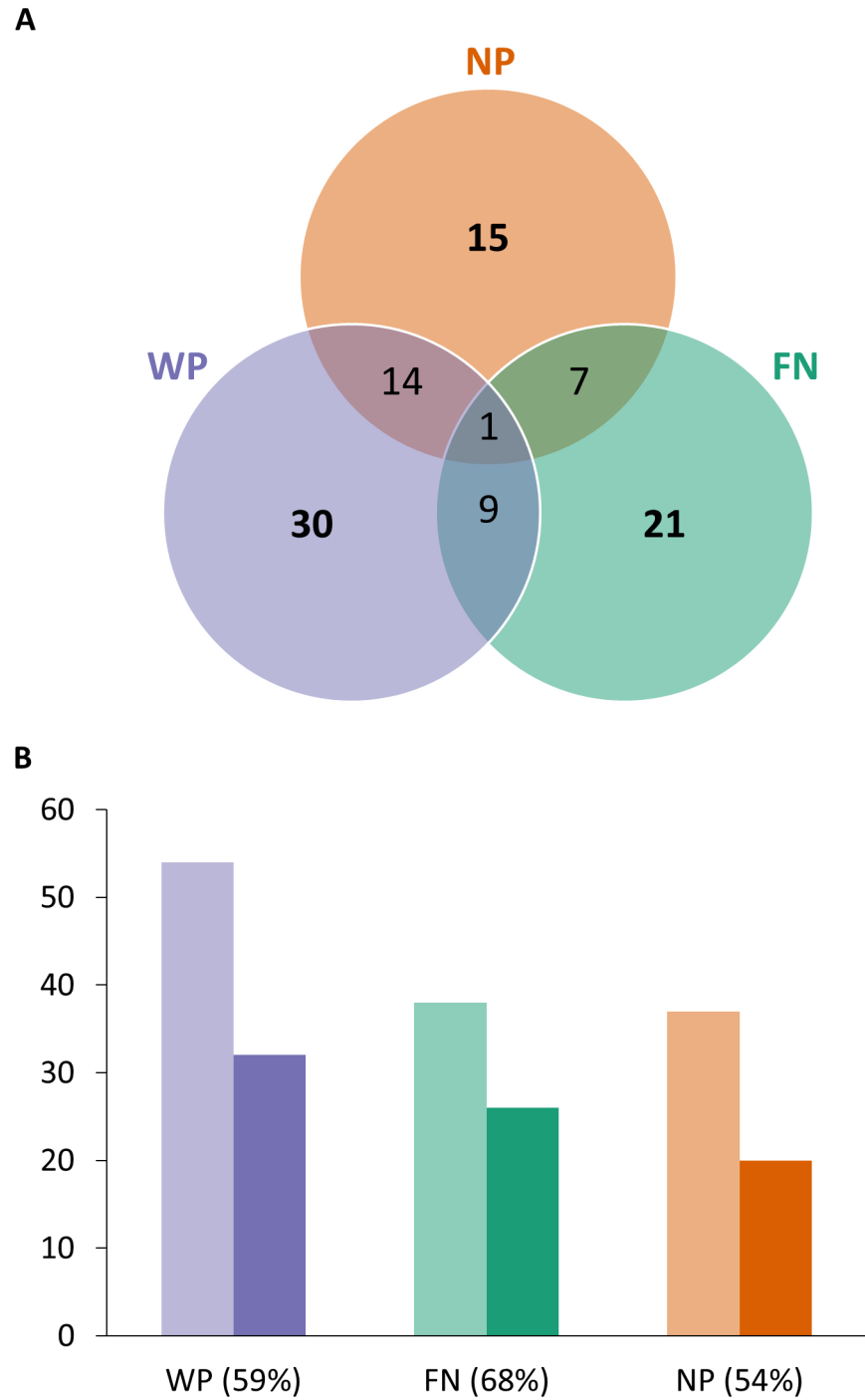


Fig 1. Signatures of selection in the Tasmanian devil genome. Ninety-seven signatures of selection were identified in the Tasmanian devil (*Sarcophilus harrisii*). Their distribution among the three investigated populations is provided in the form of (A) a Venn diagram and (B) bar plots. Light bars show the total number of signatures of selection identified in each population, among which dark bars (and the proportions between brackets) represent those standing at less than 100 kb from a protein-coding gene having a human orthologue according to Ensembl 90. Populations: FN = Freycinet; NP = Narawntapu; WP = West Pencil Pine.

<https://doi.org/10.1371/journal.pone.0201838.g001>

Table 1. Genomic time-series investigated to identify signatures of selection in the Tasmanian devil (*Sarcophilus harrisii*).

Population symbol	Sampling location	DFTD arrival	N_e	$N_1 (t_1)^a$	$N_2 (t_2)^a$	$N_3 (t_3)^a$	Nb. of analyzed SNPs	Nb. of candidate SNPs	Prop. of candidate SNPs (%)
FN	Freycinet	2001	34	29 (1999)	-	20 (2012–2013)	16978	210	1.2
NP	Narawntapu	2007	37	26 (1999)	26 (2004)	27 (2009)	27173	104	0.4
WP	West Pencil Pine	2006	26	21 (2006)	-	43 (2013–2014)	5401	88	1.6

N_e , effective population size

^a Time-series include either two (for FN and WP) or three (for NP) temporal samples. N_i denotes the size of each temporal sample i indexed in chronological order. The year of sampling, t_i , is provided between brackets.

N.B. Data were made publicly available in [13]. More information about the dataset can be found in [14].

<https://doi.org/10.1371/journal.pone.0201838.t001>

genes. The top molecular and cellular functions included several “cell-related functions” such as cell cycle, morphology and organization. Other functions were related to nucleic acids, primary metabolism and the immune system, as shown in Fig 2. Among the top 100 disease-related categories, 73 were associated with “cancer” (S2 Table). The “solid tumor” category was the most overrepresented (p -value = 1.16×10^{-10} , FDR = 4.39×10^{-7}) with 138 genes out of 147 associated with this term. According to IPA, all the 60 signatures of selection were located in the vicinity of coding sequence host genes potentially related to cancer.

Some candidate genes are key regulators of signaling pathways mediating cancer progression involved in cell cycle, apoptosis and genome instability. Among these candidates are the DTWD1, NEK6 and NSD3 genes that are regulators of the G2/M transition [16–18], and BAG4 and TRIM66, which prevent apoptosis [19,20]. The CEP131 and PINX1 genes are involved in chromosome stability [21,22].

A great number of candidate genes are associated with signaling pathways that usually mediate embryonic development but may also have a role in cancer progression. Alterations of the FGFR1 gene, a tyrosine-kinase receptor (RTK), have been described in many tumors

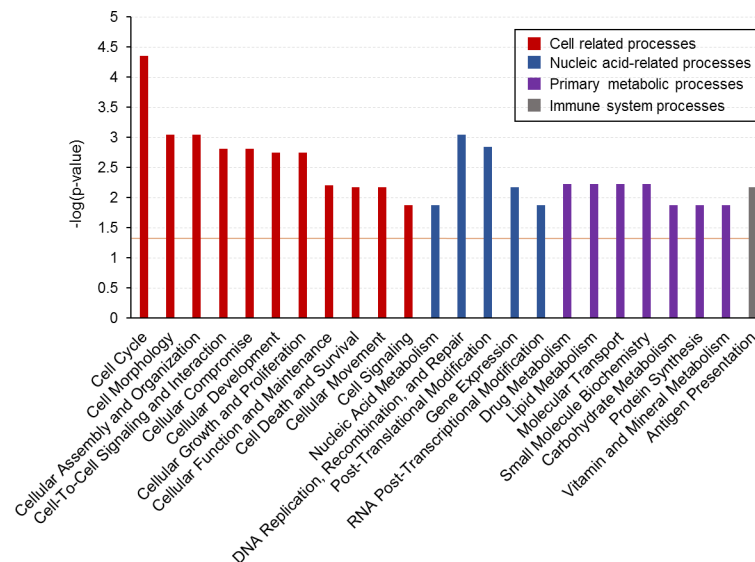


Fig 2. Molecular and functional categories associated with protein coding candidate genes. Representation of overrepresented molecular and functional categories obtained by functional analysis in IPA. Related functional categories are represented with the same color code. Only functions with a $-\log_{10}(p\text{-value}) \geq 1.3$ (orange line in the graph, corresponding to a $p\text{-value} \leq 0.05$) were considered.

<https://doi.org/10.1371/journal.pone.0201838.g002>

[23,24]. Other candidate genes are known to be involved in oncogenic RTK pathways, such as SHC4 [25] and ST5/DENND2B [26]. The CEP131 gene is involved in cell proliferation and migration through the activation of the phosphoinositide 3-kinase (PI3K/Akt) signaling [27] and the SMAD3 gene is a key mediator of the transforming growth factor- β (TGF- β) signaling pathway involved in cancer progression [28]. The candidate FOXN3 is a key gene of the Wnt/ β -Catenin pathway that is altered in cancers [29]. Other candidates, such as the SPTBN1, NSD3 and CDK14 genes, are able to influence cancer progression through Wnt signaling [18,30,31]. Key mediators of other pathways related to both development and cancer, such as Notch and Hippo, were among our candidates. The NOTCH2 gene is involved in the direct cell-cell interactions of the Notch pathway that can inhibit cancer progression [32]. The TEAD4 gene belongs to the TEAD (transcriptional enhancer factor domain) transcription factors that are required for activating the proliferation genes targeted by Hippo signaling in cancer [33].

An important subset of candidate genes are mediators of metastasis

It is noteworthy that a great number of candidate genes identified in the present study have the potential to influence invasiveness and metastasis of cancer cells. In particular, we identified seven metastasis-related genes that encode adhesion molecules (ADGRA2, ADGRD2, CDH8, MCAM, THY1, TSPAN9, and TSPAN11). Other candidates, such as PRRX2 and CST3, confer metastatic properties to cancer cells through the TGF- β pathway [34,35]. Similarly, FOXN3 [36], HMGCS2 [37], LSM1 [38], PHGDH [39], RIN2 [40], TRPM8[41], are known regulators of metastatic processes. In total, over 30 selection candidates identified in this study are known to participate in metastasis-related mechanisms.

Behavior-related genes among the identified candidate genes

The second major functional category associated with our candidate genes refers to the architecture of complex behaviors. Functions associated with development and the nervous system (S2 Table) were revealed by IPA analysis. In particular, 16 candidates were classed within the annotation term “development of neurons” (S2 Fig). Several of them may contribute to the development and homeostasis of important cellular compartments in the central nervous system (CNS). For example, SYNDIG1 is essential for the formation of excitatory synapses in the hippocampus [42]. NKX2-2 is a key regulator of serotonergic neuron development [43]. SDK2 is an adhesion molecule that regulates synaptic connections, thereby influencing the arrangement of neural circuits in the CNS [44]. KIF13B, a member of the kinesin motor protein superfamily, has a key role in the regulation of axon development [45]. Other candidates have putative roles at the synapse level. SLITRK5 and SLC38A10 play important roles in neurotransmission [46,47]. CDC42EP4 and HERC1 are involved in synapse homeostasis [48,49]. In addition, the candidate list harbors several genes encoding subunits of ion channels (e.g., CACNB2, KCNA4, KCNIP3, or KCTD3) that are involved in signal transmission in the CNS.

Some human homologues of our candidate genes are also associated with behavioral disorders. For example, the large signature of selection displayed on scaffold GL834709 (nucleotides 2,702,597 to 2,946,330) corresponds to human locus 8p11.23, which is related to cancer [50], but has also been proposed as a “neurodevelopmental hub” associated with autism spectrum disorders (ASD) according to a recent meta-analysis [51]. The NDUFAF5 candidate is involved in the assembly of the first complex of the respiratory chain [52], which is frequently impaired in CNS disorders like ASD [53]. Several other candidates, such as CACNB2 [54], CDH8 [55], HERC1 [56], KCTD3 [57], KIF13B [58], SERINC2 [59], and SLC39A11 [60] have been associated with ASD. Some candidates have been linked to intellectual disability (ID),

such as CRBN [61], GPKOW [62], HERC1 [56] and KCNA4 [63], or to other behavioral disorders, such as CDC42EP4 [64] and SLITRK5 [46].

A few candidates may contribute to immunity

Immunity, a function that may be related to cancer progression, is also represented through a few genes. In particular, six candidates (TRIM10, TRIM15, TRIM26, TRIM39-RPP21, TRIM62, and TRIM66) are members of the large tripartite motif (TRIM) family that consists of ubiquitin ligases involved in both innate immunity and cancer progression [65]. With the exception of TRIM39-RPP21, all the TRIM genes identified here are known to be related to cancer according to IPA (S1 Table). TRIM10, TRIM15, TRIM26, and TRIM39-RPP21 belong to the human leukocyte antigen (HLA) region, which gathers many immunity regulators [66]. TRIM62 and TRIM66 have also been suggested to have a role in immunity [67,68]. Candidates from the TSPAN (TSPAN9, TSPAN11) and the aGPCR (ADGRA2, ADGRD2) families, which were cited above for their putative roles in metastasis, may also be implicated in immune response [69,70]. The versatile SMAD3 candidate has been shown to influence the immunosurveillance of cancer [71].

Discussion

The Tasmanian devil dataset investigated here was initially presented and analyzed by Epstein et al. [14], who reported two putatively selected regions harboring seven candidate genes. These two regions were also detected in our analysis and correspond to signatures of selection located in scaffolds GL841593 (nucleotides 4,501,785 to 4,979,756) and GL849657 (nucleotides 283,671 to 283,701). Epstein et al. [14] performed their analysis with a composite test statistic that took into account temporal changes in both allele frequency and integrated extended haplotype homozygosity of an individual SNP site (iES) [72]. Such an approach is based on the idea that an SNP undergoing strong selection would rapidly rise in frequency, while the haplotypic diversity of the surrounding region would suddenly decrease. To avoid false-positives, Epstein et al. [14] restricted their analysis to the candidate regions shared by the three populations. The limit of this approach is that the total number of candidate genes detectable is highly dependent on the SNP density, especially since the West Pencil Pine (WP) population presented a low genotyping density with only ~ 5000 available SNP (Table 1).

We chose a different approach than that proposed in [14]. First, the three devil populations were analyzed separately since there is substantial genotyping heterogeneity among populations (Table 1). In addition, the genetic structuration of the Tasmanian devil implies that some observed polymorphisms are expected to be population-specific [10,12]. In particular, the existence of population-specific genotypes has already been emphasized to account for some phenotypic differences in response to DFTD among devil populations [73]. Second, we used a customized method that looks for selection in each population independently. Our method is based on a Wright-Fisher model coupled to maximum-likelihood computations, which makes it possible to determine whether the observed temporal variation in SNP frequency is more likely to be caused by selection and drift than by drift alone in each population. Importantly, our method implements a test statistic that takes into account the amount of drift through the effective population size (N_e), in each population. Despite the very low N_e in the Tasmanian devil ($N_e \sim 30$, see [14]), our method allowed the identification of 97 signatures of selection (Fig 1A). This confirms that the selection imposed to the Tasmanian devil during the emergence of DFTD was extremely intense and that the evolutionary response to a transmissible cancer may involve the contribution of many genes, which is in line with the complex multi-step processes of cancer [74].

Our analysis identified a majority of population-specific candidate regions for DFTD-linked selection (Fig 1A). The low number of candidate regions overlapping among populations may be explained by different factors. The first relates to the large sampling heterogeneity in genotyping and in SNP densities among populations, as demonstrated by the fact that only 5% of the SNPs were common among populations. The second reason involves the complex host-cancer interaction, which strongly depends on the genetic variation available in the host population. We can expect selection to act on different genes in different populations because between-population genetic variation exists. This does not necessarily imply that the adaptive mechanisms selected to resist cancer are dramatically different among devil populations; rather, this refers to the redundancy of gene functions, with different genes or different pathways being able to act in a similar and functional manner [75].

The Tasmanian devil-DFTD interaction is a nice example of host-pathogen reciprocal evolutionary process. DFTD-driven selection acts to increase host resistance and reduce the negative effects of the tumor on individual fitness. In an evolutionary antagonistic process, DFTD evolves to counter-adapt in response to the host adaptive changes [76]. Our study, as in the previous analysis by Epstein et al. [14], focuses on the genetic changes arising in the host, rather than the tumor itself.

DFTD-driven selection has targeted genes in the host cells of the tumor microenvironment [77,78], where non-cancerous cells such as fibroblasts, adipocytes, inflammatory cells, etc., contribute to the malignant progression [79]. Genes selected in the host may therefore limit normal cell recruitment and activation by the cancerous cells [80], and regulate metastasis-related processes [81,82].

Through our analysis, we identified more than 30 candidate genes that may contribute to metastasis. In particular, some of them belong to different families of cell adhesion molecules (e.g., tetraspanins, cadherins, adhesion G protein-coupled receptors, immunoglobulins), which are essential in processes that lead to metastasis [83]. For example, both MCAM and THY1, which encode cell adhesion molecules of the immunoglobulin superfamily (IgSF-CAMs), are frequently overexpressed in metastatic tumor tissues [84,85]. Moreover, tetraspanins and adhesion G protein-coupled receptors also influence metastasis [86–88] as well as the cadherin CDH8 [89]. These results must be considered in the light of the high prevalence of DFTD metastases in infected devils [7] and the importance of cell adhesion processes in shaping the tumor microenvironment [82]. All this suggests that the control of metastasis, in particular through the maintenance of the host tissue integrity, could be an essential component of the host evolutionary response to DFTD.

In addition to the strong association with metastasis mentioned above, the functional annotation of our candidate genes allowed identifying putative key mediators of cellular processes frequently deregulated in cancers, such as cell cycle control and apoptosis. Well-known signaling pathways related to both cancer and development, such as MAP-kinase, TGF- β and Wnt pathways, were also targeted by selection. In a marsupial such as the Tasmanian devil, the development of neonates represents a critical window for selection [90]. As a consequence, we must consider the possibility that selection has targeted some genes for their developmental role or even for their specific tumor-suppressive action during development [90].

Overall, our analysis suggests that natural selection may have targeted multiple cellular circuits to limit the acquisition of cancerous features in devil tumor tissues [74,79], which should ultimately prevent or at least delay cancer growth and metastatic processes. In the context of a transmissible cancer, such genetic changes are expected to provide the host with increased fitness, since host individuals with a slow DFTD progression will be able to reproduce despite infection [9,91].

Among the target genes identified in this study, there are several human orthologues associated with behavioral disorders affecting synaptic connections and characterized by deficits in communication and social interaction, such as ASD and ID [92–94]. This observation is very intriguing, especially in the light of recent results indicating that more aggressive individuals were at greater risk of developing DFTD [11,91,95]. DFTD-driven selection could therefore have favored less aggressive individuals, which are less likely to be infected due to reduced physical interactions with other Tasmanian devils [91]. This empirically supports the hypothesis recently discussed in [2] that an evolutionary response to cancer could rely not only on cellular pathways involved in cancer progression, but also on adjustments of life-history traits and behavior. Even if evolutionary costs driven by sexual selection may be opposed—because socially dominant individuals engage more often in mating [91]—, Roche et al. [2] suggest that “the avoidance of contagious cancers could be a selective force for specific behavior”, which agrees with our results. The Tasmanian devil-DFTD interaction provides a good natural model for further investigating this hypothesis through additional field and resequencing studies.

Overall, our results suggest that DFTD has extensively shaped the genome of the Tasmanian devil and that several functions have been targeted in the host by DFTD-driven selection. This supports the evidence that adaptation occurs rapidly even in situations of limited genetic variation. Our study also shows that genomic time-series data are particularly useful for detecting signatures of selection associated with complex phenotypes even when the number of generations of selection investigated (~ 5 generations) and the effective population size ($N_e \sim 30$) are very small. In this study, we only had the opportunity to explore the host perspective of the host-tumor interaction. Further studies incorporating genomic time-series data from both the host and the transmissible tumor will be required to better understand the host-tumor coevolution.

Methods

Tasmanian devil dataset

The data analyzed in the present article were initially reported in [14] and made publicly available as a Dryad data package [13]. This data package consists of SNP genotyping data produced by Stacks [96] following RAD-seq (Restriction-site Associated DNA sequencing) assays [97] from tissue samples collected in 360 Tasmanian devils across Tasmania. Samples were collected at different time points between 1999 and 2014, allowing the analysis of genomic time-series that take into account the impact of DFTD through time on Tasmanian devil populations. We restricted our analysis to the same samples as in [14], from the localities of Freycinet (FN), Narawntapu (NP) and West Pencil Pine (WP). We reproduced the SNP filtering strategy reported in [14]. In brief, we performed filtering according to (i) MAF computed over the whole dataset (SNP with MAF less than 0.01 were discarded), (ii) observed heterozygosity computed over the whole dataset (SNP with heterozygosity over 0.5 were discarded), (iii) the proportion of missing genotypes (SNP with less than one-third of genotypes either in the whole dataset or in a sample were discarded, except for the two smallest samples in which SNP with less than half genotypes were removed), (iv) the linkage disequilibrium between neighboring SNP (using PLINK [98], we removed one SNP from pairs of SNP harboring $R^2 > 0.99$ over 20 successive SNP and 50 kb of distance in any sample). We obtained filtered datasets of 16978, 27173 and 5401 SNP for the FN, NP and WP populations, respectively. Relevant information about the dataset for the present work is summarized in Table 1. Further information about sample collection, genotyping and data processing can be found in [14].

Signatures of selection

We submitted the genomic time-series of the three investigated Tasmanian devil populations to a customized method for detecting footprints of selection (available at <https://github.com/hubert-pop/signasel>). This method was initially described and successfully implemented to detect genomic regions targeted by short-term selection in experimental wheat populations [15]. Briefly, this method compares two Wright-Fisher models, one including drift and the other including drift plus selection, in a maximum-likelihood framework. The model that best fits the SNP frequency variation observed over time is identified through a Likelihood Ratio Test (LRT). Each SNP is individually tested and associated with a p-value that quantifies to what extent the temporal variation in SNP frequency may be due to selection, under a null hypothesis postulating an effect of drift only. A strength of this method is to model and disentangle the effects of drift plus selection as opposed to those of drift alone in a population-specific manner. This has proven to be efficient for detecting SNP under selection from genomic temporal samples separated by a few generations in small populations undergoing intense selection, as in the Tasmanian devil. For example, we performed simulations mimicking a strong selection (applying a constant selection coefficient of 0.5) in the FN population (considering a constant effective population size, N_e , of 34, and a sampling interval of 6 generations). In such a case, the power to detect a truly selected SNP was 61%, while the false-positive rate was about 1%, suggesting that our method would provide enough power to find signatures of selection from the Tasmanian devil dataset. In the real data analysis, we corrected for multiple testing by applying the Benjamini-Hochberg false-discovery rate (FDR) procedure [99]. Therefore, we considered as relevant signatures of selection the genomic regions that included at least one SNP with a p-value < 0.0001 (which corresponds to a FDR of $\sim 8\%$) or at least two neighboring SNP with p-values < 0.01 (which corresponds to a FDR of $\sim 13.5\%$). We looked for candidates for selection by applying our method to two temporal samples in the FN (the sample from 1999 and the combination of those from 2012 and 2013) and WP (the sample from 2006 and the combination of those from 2013 and 2014) populations, and to three temporal samples (samples from 1999, 2004 and 2009) in the NP population (Table 1). Given the sampling times and an assumed generation time of 2 years in the Tasmanian devil [14], we considered that the time-series covered a period of 6, 5, and 3 complete generations in the FN, NP, and WP populations, respectively. As our method relies on Wright-Fisher models, the effective size (N_e) of each investigated population must be provided. Simulations indicated that a bias in the estimation of N_e may under some circumstances affect the power to detect selection but has almost no impact on the false-positive rate (data not shown). We used the values of N_e suggested in [14], that is, 34, 37 and 26 for the FN, NP and WP populations, respectively. These estimates come from the Jorde and Ryman method [100] for inferring unbiased contemporary N_e from genetic data.

Candidate gene identification

We identified as candidate genes all the protein coding genes standing at less than 100 kb from the detected signatures of selection and having a human orthologue according to the Ensembl genome browser 90 (<https://www.ensembl.org>). Ensembl stable ID of candidate genes and corresponding orthologues were retrieved using the Ensembl Genes 90 database and the Devil_ref v7.0 Tasmanian devil reference assembly [101] obtained from BioMart.

Ingenuity pathway analysis

We used the manually curated database IPA® (Ingenuity Pathway Analysis, QIAGEN Inc., <https://www.qiagenbioinformatics.com/products/ingenuity-pathway-analysis>) to identify the

diseases and developmental disorder as well as the molecular and cellular functions associated with our candidate genes. We submitted the list of 147 human orthologues of our candidate genes to a “Core Analysis” with the “Ingenuity Knowledge Base” reference set to find overrepresented functions and diseases in our gene set. This is achieved by IPA by applying a right-tailed Fisher Exact test to estimate the likelihood that the overlap between the set of genes and a given function or disease is due to random chance.

Supporting information

S1 Fig. Sixty signatures of selection were identified in 53 scaffolds in the Tasmanian devil genome at less than 100 kb from a protein coding gene having a human orthologue.

(PDF)

S2 Fig. Sixteen candidate genes are associated with the annotation term ‘development of neurons’.

(TIFF)

S1 Table. List of candidate genes for DFTD-driven selection in the Tasmanian devil.

(XLSX)

S2 Table. Top hundred annotation terms associated by IPA with the list of candidate genes.

(XLSX)

Acknowledgments

The authors wish to thank Wendy Brand-Williams for linguistic revision of the manuscript and Andrea Rau for useful suggestions.

Author Contributions

Formal analysis: Jean-Noël Hubert, Tatiana Zerjal.

Investigation: Jean-Noël Hubert.

Methodology: Frédéric Hospital.

Software: Jean-Noël Hubert, Frédéric Hospital.

Supervision: Frédéric Hospital.

Visualization: Jean-Noël Hubert, Tatiana Zerjal.

Writing – original draft: Jean-Noël Hubert, Tatiana Zerjal.

Writing – review & editing: Jean-Noël Hubert, Tatiana Zerjal, Frédéric Hospital.

References

1. Schiffman JD, Breen M. Comparative oncology: what dogs and other species can teach us about humans with cancer. *Philos Trans R Soc Lond B Biol Sci.* 2015; 370(1673). <https://doi.org/10.1098/rstb.2014.0231> PMID: 26056372
2. Roche B, Moller AP, de Gregori J, Thomas F. Cancer in animals: reciprocal feedbacks between evolution of cancer resistance and ecosystem functioning. In: Ujvari B, Roche B, Thomas F, editors. *Ecology and Evolution of Cancer.* 2017. pp. 180–188.
3. Murchison EP, Wedge DC, Alexandrov LB, Fu B, Martincorena I, Ning Z, et al. Transmissible dog cancer genome reveals the origin and history of an ancient cell lineage. *Science.* 2014; 343(6169), 437–440. <https://doi.org/10.1126/science.1247167> PMID: 24458646

4. Hawkins CE, Baars C, Hesterman H, Hocking GJ, Jones ME, Lazenby B, et al. Emerging disease and population decline of an island endemic, the Tasmanian devil *Sarcophilus harrisii*. *Biol Conserv*. 2006; 131(2): 307–324.
5. Metzger MJ, Villalba A, Carballal MJ, Iglesias D, Sherry J, Reinisch C, et al. Widespread transmission of independent cancer lineages within multiple bivalve species. *Nature*. 2016; 534(7609): 705–9. <https://doi.org/10.1038/nature18599> PMID: 27338791
6. McCallum H, Jones M, Hawkins C, Hamede R, Lachish S, Sinn DL, et al. Transmission dynamics of Tasmanian devil facial tumor disease may lead to disease-induced extinction. *Ecology*. 2009; 90(12): 3379–92. PMID: 20120807
7. Belov K. Contagious cancer: lessons from the devil and the dog. *Bioessays*. 2012; 34(4): 285–92. <https://doi.org/10.1002/bies.201100161> PMID: 22383221
8. Pye RJ, Woods GM, Kreiss A. Devil facial tumor disease. *Vet Pathol*. 2016; 53(4): 726–36. <https://doi.org/10.1177/0300985815616444> PMID: 26657222
9. Pye RJ, Hamede R, Siddle HV, Caldwell A, Knowles GW, Swift K, et al. Demonstration of immune responses against devil facial tumour disease in wild Tasmanian devils. *Biol Lett*. 2016; 12(10). <https://doi.org/10.1098/rsbl.2016.0553> PMID: 28120799
10. Storfer A, Epstein B, Jones M, Micheletti S, Spear SF, Lachish S, et al. Landscape genetics of the Tasmanian devil: implications for spread of an infectious cancer. *Conserv Genet*. 2017; 18(6): 1287–1297.
11. Hamede RK, McCallum H, Jones M. Biting injuries and transmission of Tasmanian devil facial tumour disease. *J Anim Ecol*. 2013; 82(1): 182–90. <https://doi.org/10.1111/j.1365-2656.2012.02025.x> PMID: 22943286
12. Hendricks S, Epstein B, Schönfeld B, Wiench C, Hamede R, Jones M, et al. Conservation implications of limited genetic diversity and population structure in Tasmanian devils (*Sarcophilus harrisii*). *Conserv Genet*. 2017; 18(4): 977–982. <https://doi.org/10.1007/s10592-017-0939-5> PMID: 28966567
13. Epstein B, Jones M, Hamede R, Hendricks S, McCallum H, Murchison EP, et al. Rapid evolutionary response to a transmissible cancer in Tasmanian devils. *Dryad Digital Repository*. 2016. <http://dx.doi.org/10.5061/dryad.r60sv>
14. Epstein B, Jones M, Hamede R, Hendricks S, McCallum H, Murchison EP, et al. Rapid evolutionary response to a transmissible cancer in Tasmanian devils. *Nat Commun*. 2016; 7: 12684. <https://doi.org/10.1038/ncomms12684> PMID: 27575253
15. Thépot S, Restoux G, Goldringer I, Gouache D, Hospital F, Mackay I, et al. Efficiently tracking selection in a multiparental population: the case of earliness in wheat. *Genetics*. 2015; 199(2): 609–23. <https://doi.org/10.1534/genetics.114.169995> PMID: 25406468
16. Zhang B, Zhang H, Wang D, Han S, Wang K, Yao A, et al. Never in mitosis gene A-related kinase 6 promotes cell proliferation of hepatocellular carcinoma via cyclin B modulation. *Oncol Lett*. 2014; 8(3): 1163–1168. <https://doi.org/10.3892/ol.2014.2300> PMID: 25120679
17. Ma Y, Yue Y, Pan M, Sun J, Chu J, Lin X, et al. Histone deacetylase 3 inhibits new tumor suppressor gene DTWD1 in gastric cancer. *Am J Cancer Res*. 2015; 5(2): 663–73. PMID: 25973305
18. Vougiouklakis T, Hamamoto R, Nakamura Y, Saloura V. The NSD family of protein methyltransferases in human cancer. *Epigenomics*. 2015; 7(5): 863–74. <https://doi.org/10.2217/epi.15.32> PMID: 25942451
19. Jiang Y, Woronicz JD, Liu W, Goeddel DV. Prevention of constitutive TNF receptor 1 signaling by silencer of death domains. *Science*. 1999; 283(5401): 543–6. PMID: 9915703
20. Chen Y, Guo Y, Yang H, Shi G, Xu G, Shi J, et al. TRIM66 overexpression contributes to osteosarcoma carcinogenesis and indicates poor survival outcome. *Oncotarget*. 2015; 6(27): 23708–19. <https://doi.org/10.18632/oncotarget.4291> PMID: 26247633
21. Staples CJ, Myers KN, Beveridge RD, Patil AA, Lee AJ, Swanton C, et al. The centriolar satellite protein Cep131 is important for genome stability. *J Cell Sci*. 2012; 125(Pt 20): 4770–9. <https://doi.org/10.1242/jcs.104059> PMID: 22797915
22. Li HL, Song J, Yong HM, Hou PF, Chen YS, Song WB, et al. PinX1: structure, regulation and its functions in cancer. *Oncotarget*. 2016; 7(40): 66267–66275. <https://doi.org/10.18632/oncotarget.11411> PMID: 27556185
23. Jones DT, Hutter B, Jäger N, Korshunov A, Kool M, Warnatz HJ, et al. Recurrent somatic alterations of FGFR1 and NTRK2 in pilocytic astrocytoma. *Nat Genet*. 2013; 45(8): 927–32. <https://doi.org/10.1038/ng.2682> PMID: 23817572
24. Cowell JK, Qin H, Hu T, Wu Q, Bhole A, Ren M. Mutation in the FGFR1 tyrosine kinase domain or inactivation of PTEN is associated with acquired resistance to FGFR inhibitors in FGFR1-driven leukemia/

- lymphomas. *Int J Cancer*. 2017; 141(9): 1822–1829. <https://doi.org/10.1002/ijc.30848> PMID: 28646488
25. Strub T, Kobi D, Koludrovic D, Davidson I. A POU3F2-MITF-SHC4 axis in phenotype switching of melanoma cells. In: Murph M, editor. *Research on Melanoma—A Glimpse into Current Directions and Future Trends*. 2011. <https://doi.org/10.5772/19769>
 26. Ioannou MS, McPherson PS. Regulation of cancer cell behavior by the small GTPase Rab13. *J Biol Chem*. 2016; 291(19): 9929–37. <https://doi.org/10.1074/jbc.R116.715193> PMID: 27044746
 27. Liu XH, Yang YF, Fang HY, Wang XH, Zhang MF, Wu DC. CEP131 indicates poor prognosis and promotes cell proliferation and migration in hepatocellular carcinoma. *Int J Biochem Cell Biol*. 2017; 90: 1–8. <https://doi.org/10.1016/j.biocel.2017.07.001> PMID: 28694105
 28. Syed V. TGF- β Signaling in Cancer. *J Cell Biochem*. 2016; 117(6): 1279–87. <https://doi.org/10.1002/jcb.25496> PMID: 26774024
 29. Nusse R, Clevers H. Wnt/ β -Catenin Signaling, Disease, and Emerging Therapeutic Modalities. *Cell*. 2017; 169(6): 985–999. <https://doi.org/10.1016/j.cell.2017.05.016> PMID: 28575679
 30. Davidson G, Niehrs C. Emerging links between CDK cell cycle regulators and Wnt signaling. *Trends Cell Biol*. 2010; 20(8): 453–60. <https://doi.org/10.1016/j.tcb.2010.05.002> PMID: 20627573
 31. Zhi X, Lin L, Yang S, Bhuvaneshwar K, Wang H, Gusev Y, et al. β II-Spectrin (SPTBN1) suppresses progression of hepatocellular carcinoma and Wnt signaling by regulation of Wnt inhibitor kallistatin. *Hepatology*. 2015; 61(2): 598–612. <https://doi.org/10.1002/hep.27558> PMID: 25307947
 32. Nowell CS, Radtke F. Notch as a tumour suppressor. *Nat Rev Cancer*. 2017; 17(3): 145–159. <https://doi.org/10.1038/nrc.2016.145> PMID: 28154375
 33. Harvey KF, Zhang X, Thomas DM. The Hippo pathway and human cancer. *Nat Rev Cancer*. 2013; 13(4): 246–57. <https://doi.org/10.1038/nrc3458> PMID: 23467301
 34. Juang YL, Jeng YM, Chen CL, Lien HC. PRRX2 as a novel TGF- β -induced factor enhances invasion and migration in mammary epithelial cell and correlates with poor prognosis in breast cancer. *Mol Carcinog*. 2016; 55(12): 2247–2259. <https://doi.org/10.1002/mc.22465> PMID: 26824226
 35. Yan Y, Fan Q, Wang L, Zhou Y, Li J, Zhou K. LncRNA Snhg1, a non-degradable sponge for miR-338, promotes expression of proto-oncogene CST3 in primary esophageal cancer cells. *Oncotarget*. 2017; 8(22): 35750–35760. <https://doi.org/10.18632/oncotarget.16189> PMID: 28423738
 36. Dai Y, Wang M, Wu H, Xiao M, Liu H, Zhang D. Loss of FOXN3 in colon cancer activates beta-catenin/TCF signaling and promotes the growth and migration of cancer cells. *Oncotarget*. 2017; 8(6): 9783–9793. <https://doi.org/10.18632/oncotarget.14189> PMID: 28039460
 37. Chen SW, Chou CT, Chang CC, Li YJ, Chen ST, Lin IC, et al. HMGCS2 enhances invasion and metastasis via direct interaction with PPAR α to activate Src signaling in colorectal cancer and oral cancer. *Oncotarget*. 2017; 8(14): 22460–22476. <https://doi.org/10.18632/oncotarget.13006> PMID: 27816970
 38. Little EC, Camp ER, Wang C, Watson PM, Watson DK, Cole DJ. The CaSm (LSm1) oncogene promotes transformation, chemoresistance and metastasis of pancreatic cancer cells. *Oncogenesis*. 2016; 5: e182. <https://doi.org/10.1038/oncsis.2015.45> PMID: 26751936
 39. Samanta D, Park Y, Andrabi SA, Shelton LM, Gilkes DM, Semenza GL. PHGDH expression is required for mitochondrial redox homeostasis, breast cancer stem cell maintenance, and lung metastasis. *Cancer Res*. 2016; 76(15): 4430–42. <https://doi.org/10.1158/0008-5472.CAN-16-0530> PMID: 27280394
 40. Sandri C, Caccavari F, Valdembrì D, Camillo C, Vettel S, Santambrogio M, et al. The R-Ras/RIN2/Rab5 complex controls endothelial cell adhesion and morphogenesis via active integrin endocytosis and Rac signaling. *Cell Res*. 2012; 22(10): 1479–501. <https://doi.org/10.1038/cr.2012.110> PMID: 22825554
 41. Yee NS. Roles of TRPM8 ion channels in cancer: proliferation, survival, and invasion. *Cancers (Basel)*. 2015; 7(4): 2134–46. <https://doi.org/10.3390/cancers7040882> PMID: 26512697
 42. Lovero KL, Blankenship SM, Shi Y, Nicoll RA. SynDIG1 promotes excitatory synaptogenesis independent of AMPA receptor trafficking and biophysical regulation. *PLoS One*. 2013; 8(6): e66171. <https://doi.org/10.1371/journal.pone.0066171> PMID: 23785483
 43. Cheng L, Chen CL, Luo P, Tan M, Qiu M, Johnson R, et al. Lmx1b, Pet-1, and Nkx2.2 coordinately specify serotonergic neurotransmitter phenotype. *J Neurosci*. 2003; 23(31): 9961–7. PMID: 14602809
 44. Krishnaswamy A, Yamagata M, Duan X, Hong YK, Sanes JR. Sidekick 2 directs formation of a retinal circuit that detects differential motion. *Nature*. 2015; 524(7566): 466–470. <https://doi.org/10.1038/nature14682> PMID: 26287463

45. Nakata T, Hirokawa N. Neuronal polarity and the kinesin superfamily proteins. *Sci STKE*. 2007; 2007(372): pe6. <https://doi.org/10.1126/stke.3722007pe6> PMID: 17284724
46. Shmelkov SV, Hormigo A, Jing D, Proenca CC, Bath KG, Milde T, et al. *Slitrk5* deficiency impairs corticostriatal circuitry and leads to obsessive-compulsive-like behaviors in mice. *Nat Med*. 2010; 16(5): 598–602, 1p following 602. <https://doi.org/10.1038/nm.2125> PMID: 20418887
47. Hellsten SV, Hägglund MG, Eriksson MM, Fredriksson R. The neuronal and astrocytic protein SLC38A10 transports glutamine, glutamate, and aspartate, suggesting a role in neurotransmission. *FEBS Open Bio*. 2017; 7(6): 730–746. <https://doi.org/10.1002/2211-5463.12219> PMID: 28593130
48. Ageta-Ishihara N, Yamazaki M, Konno K, Nakayama H, Abe M, Hashimoto K, et al. CDC42EP4/septin-based perisynaptic glial scaffold facilitates glutamate clearance. *Nat Commun*. 2015; 6: 10090. <https://doi.org/10.1038/ncomms10090> PMID: 26657011
49. Bachiller S, Rybkina T, Porras-García E, Pérez-Villegas E, Tabares L, Armengol JA, et al. The HERC1 E3 ubiquitin ligase is essential for normal development and for neurotransmission at the mouse neuromuscular junction. *Cell Mol Life Sci*. 2015; 72(15): 2961–71. <https://doi.org/10.1007/s00018-015-1878-2> PMID: 25746226
50. Garcia MJ, Pole JC, Chin SF, Teschendorff A, Naderi A, Ozdag H, et al. A 1 Mb minimal amplicon at 8p11-12 in breast cancer identifies new candidate oncogenes. *Oncogene*. 2005; 24(33): 5235–45. <https://doi.org/10.1038/sj.onc.1208741> PMID: 15897872
51. Autism Spectrum Disorders Working Group of The Psychiatric Genomics Consortium, Anney RJ, Ripke S, Anttila V, Grove J, Holmans P, et al. Meta-analysis of GWAS of over 16,000 individuals with autism spectrum disorder highlights a novel locus at 10q24.32 and a significant overlap with schizophrenia. *Mol Autism*. 2017; 8: 21. <https://doi.org/10.1186/s13229-017-0137-9> PMID: 28540026
52. Rhein VF, Carroll J, Ding S, Fearnley IM, Walker JE. NDUFAF5 hydroxylates NDUFS7 at an early stage in the assembly of human complex I. *J Biol Chem*. 2016; 291(28): 14851–60. <https://doi.org/10.1074/jbc.M116.734970> PMID: 27226634
53. Hollis F, Kanellopoulos AK, Bagni C. Mitochondrial dysfunction in Autism Spectrum Disorder: clinical features and perspectives. *Curr Opin Neurobiol*. 2017; 45: 178–187. <https://doi.org/10.1016/j.conb.2017.05.018> PMID: 28628841
54. Breitenkamp AF, Matthes J, Nass RD, Sinzig J, Lehmkuhl G, Nürnberg P, et al. Rare mutations of CACNB2 found in autism spectrum disease-affected families alter calcium channel function. *PLoS One*. 2014; 9(4): e95579. <https://doi.org/10.1371/journal.pone.0095579> PMID: 24752249
55. Pagnamenta AT, Khan H, Walker S, Gerrelli D, Wing K, Bonaglia MC, et al. Rare familial 16q21 microdeletions under a linkage peak implicate cadherin 8 (CDH8) in susceptibility to autism and learning disability. *J Med Genet*. 2011; 48(1): 48–54. <https://doi.org/10.1136/jmg.2010.079426> PMID: 20972252
56. Utine GE, Taşkıran EZ, Koşukcu C, Karaosmanoğlu B, Güleray N, Doğan ÖA, et al. HERC1 mutations in idiopathic intellectual disability. *Eur J Med Genet*. 2017; 60(5): 279–283. <https://doi.org/10.1016/j.ejmg.2017.03.007> PMID: 28323226
57. Poot M, Beyer V, Schwaab I, Damatova N, van't Slot R, Prothero J, et al. Disruption of CNTNAP2 and additional structural genome changes in a boy with speech delay and autism spectrum disorder. *Neurogenetics*. 2010; 11(1): 81–9. <https://doi.org/10.1007/s10048-009-0205-1> PMID: 19582487
58. Li J, Cai T, Jiang Y, Chen H, He X, Chen C, et al. Genes with de novo mutations are shared by four neuropsychiatric disorders discovered from NPdenovo database. *Mol Psychiatry*. 2016; 21(2): 298. <https://doi.org/10.1038/mp.2015.58> PMID: 25939403
59. Hnoonual A, Thammachote W, Tim-Aroon T, Rojnueangnit K, Hansakunachai T, Sombuntham T, et al. Chromosomal microarray analysis in a cohort of underrepresented population identifies SERINC2 as a novel candidate gene for autism spectrum disorder. *Sci Rep*. 2017; 7(1): 12096. <https://doi.org/10.1038/s41598-017-12317-3> PMID: 28935972
60. Woodbury-Smith M, Paterson AD, Thiruvahindrapduram B, Lionel AC, Marshall CR, Merico D, et al. Using extended pedigrees to identify novel autism spectrum disorder (ASD) candidate genes. *Hum Genet*. 2015; 134(2): 191–201. <https://doi.org/10.1007/s00439-014-1513-6> PMID: 25432440
61. Kaufman L, Ayub M, Vincent JB. The genetic basis of non-syndromic intellectual disability: a review. *J Neurodev Disord*. 2010; 2(4): 182–209. <https://doi.org/10.1007/s11689-010-9055-2> PMID: 21124998
62. Helmsmoortel C, Vandeweyer G, Ordoukhanian P, Van Nieuwerburgh F, Van der Aa N, Kooy RF. Challenges and opportunities in the investigation of unexplained intellectual disability using family-based whole-exome sequencing. *Clin Genet*. 2015; 88(2): 140–8. <https://doi.org/10.1111/cge.12470> PMID: 25081361
63. Kaya N, Alsagob M, D'adamio MC, Al-Bakheet A, Hasan S, Muccioli M, et al. KCNA4 deficiency leads to a syndrome of abnormal striatum, congenital cataract and intellectual disability. *J Med Genet*. 2016; 53(11): 786–792. <https://doi.org/10.1136/jmedgenet-2015-103637> PMID: 27582084

64. Yan Z, Kim E, Datta D, Lewis DA, Soderling SH. Synaptic actin dysregulation, a convergent mechanism of mental disorders?. *J Neurosci*. 2016; 36(45): 11411–11417. <https://doi.org/10.1523/JNEUROSCI.2360-16.2016> PMID: 27911743
65. Hatakeyama S. TRIM family proteins: roles in autophagy, immunity, and carcinogenesis. *Trends Biochem Sci*. 2017; 42(4): 297–311. <https://doi.org/10.1016/j.tibs.2017.01.002> PMID: 28118948
66. Shiina T, Hosomichi K, Inoko H, Kulski JK. The HLA genomic loci map: expression, interaction, diversity and disease. *J Hum Genet*. 2009; 54(1): 15–39. <https://doi.org/10.1038/jhg.2008.5> PMID: 19158813
67. Versteeg GA, Rajsbaum R, Sánchez-Aparicio MT, Maestre AM, Valdiviezo J, Shi M, et al. The E3-ligase TRIM family of proteins regulates signaling pathways triggered by innate immune pattern-recognition receptors. *Immunity*. 2013; 38(2): 384–98. <https://doi.org/10.1016/j.immuni.2012.11.013> PMID: 23438823
68. Cao Z, Conway KL, Heath RJ, Rush JS, Leshchiner ES, Ramirez-Ortiz ZG, et al. Ubiquitin ligase TRIM62 regulates CARD9-mediated anti-fungal immunity and intestinal inflammation. *Immunity*. 2015; 43(4): 715–26. <https://doi.org/10.1016/j.immuni.2015.10.005> PMID: 26488816
69. Veenbergen S, van Spriël AB. Tetraspanins in the immune response against cancer. *Immunol Lett*. 2011; 138(2): 129–36. <https://doi.org/10.1016/j.imlet.2011.03.010> PMID: 21497620
70. Nijmeijer S, Vischer HF, Leurs R. Adhesion GPCRs in immunology. *Biochem Pharmacol*. 2016; 114: 88–102. <https://doi.org/10.1016/j.bcp.2016.04.013> PMID: 27131861
71. Tang PMK, Zhou S, Meng XM, Wang QM, Li CJ, Lian GY, et al. Smad3 promotes cancer progression by inhibiting E4BP4-mediated NK cell development. *Nat Commun*. 2017; 8: 14677. <https://doi.org/10.1038/ncomms14677> PMID: 28262747
72. Tang K, Thornton KR, Stoneking M. A new approach for using genome scans to detect recent positive selection in the human genome. *PLoS Biol*. 2007; 5(7): e171. <https://doi.org/10.1371/journal.pbio.0050171> PMID: 17579516
73. Hamede R, Lachish S, Belov K, Woods G, Kreiss A, Pearse AM, et al. Reduced effect of Tasmanian devil facial tumor disease at the disease front. *Conserv Biol*. 2012; 26(1): 124–34. <https://doi.org/10.1111/j.1523-1739.2011.01747.x> PMID: 21978020
74. Hanahan D, Weinberg RA. Hallmarks of cancer: the next generation. *Cell*. 2011; 144(5): 646–74. <https://doi.org/10.1016/j.cell.2011.02.013> PMID: 21376230
75. Lavi O. Redundancy: a critical obstacle to improving cancer therapy. *Cancer Res*. 2015; 75(5): 808–12. <https://doi.org/10.1158/0008-5472.CAN-14-3256> PMID: 25576083
76. Ujvari B, Pearse AM, Swift K, Hodson P, Hua B, Pyecroft S, et al. Anthropogenic selection enhances cancer evolution in Tasmanian devil tumours. *Evol Appl*. 2014; 7(2): 260–5. <https://doi.org/10.1111/eva.12117> PMID: 24567746
77. Tissot T, Arnal A, Jacqueline C, Poulin R, Lefèvre T, Mery F, et al. Host manipulation by cancer cells: Expectations, facts, and therapeutic implications. *Bioessays*. 2016; 38(3): 276–85. <https://doi.org/10.1002/bies.201500163> PMID: 26849295
78. Ujvari B, Papenfuss AT, Belov K. Transmissible cancers in an evolutionary context. *Bioessays*. 2016; 38(S1): S14–S23. <https://doi.org/10.1002/bies.201670904> PMID: 27417118
79. Hanahan D, Coussens LM. Accessories to the crime: functions of cells recruited to the tumor microenvironment. *Cancer Cell*. 2012; 21(3): 309–22. <https://doi.org/10.1016/j.ccr.2012.02.022> PMID: 22439926
80. Liao Z, Tan ZW, Zhu P, Tan NS. Cancer-associated fibroblasts in tumor microenvironment—accomplices in tumor malignancy. *Cell Immunol*. 2018. pii: S0008–8749(17)30222-8. <https://doi.org/10.1016/j.cellimm.2017.12.003> PMID: 29397066
81. Klein-Goldberg A, Maman S, Witz IP. The role played by the microenvironment in site-specific metastasis. *Cancer Lett*. 2014; 352(1): 54–8. <https://doi.org/10.1016/j.canlet.2013.08.029> PMID: 23988268
82. Salvador E, Burek M, Förster CY. Tight junctions and the tumor microenvironment. *Curr Pathobiol Rep*. 2016; 4: 135–145. <https://doi.org/10.1007/s40139-016-0106-6> PMID: 27547510
83. Li DM, Feng YM. Signaling mechanism of cell adhesion molecules in breast cancer metastasis: potential therapeutic targets. *Breast Cancer Res Treat*. 2011; 128(1): 7–21. <https://doi.org/10.1007/s10549-011-1499-x> PMID: 21499686
84. Wu Z, Wu Z, Li J, Yang X, Wang Y, Yu Y, et al. MCAM is a novel metastasis marker and regulates spreading, apoptosis and invasion of ovarian cancer cells. *Tumour Biol*. 2012; 33(5): 1619–28. <https://doi.org/10.1007/s13277-012-0417-0> PMID: 22610942
85. Zhang DH, Yang ZL, Zhou EX, Miao XY, Zou Q, Li JH, et al. Overexpression of Thy1 and ITGA6 is associated with invasion, metastasis and poor prognosis in human gallbladder carcinoma. *Oncol Lett*. 2016; 12(6): 5136–5144. <https://doi.org/10.3892/ol.2016.5341> PMID: 28105220

86. Vallon M, Essler M. Proteolytically processed soluble tumor endothelial marker (TEM) 5 mediates endothelial cell survival during angiogenesis by linking integrin $\alpha v \beta 3$ to glycosaminoglycans. *J Biol Chem*. 2006; 281(45): 34179–88. <https://doi.org/10.1074/jbc.M605291200> PMID: 16982628
87. Detchokul S, Williams ED, Parker MW, Frauman AG. Tetraspanins as regulators of the tumour micro-environment: implications for metastasis and therapeutic strategies. *Br J Pharmacol*. 2014; 171(24): 5462–90. <https://doi.org/10.1111/bph.12260> PMID: 23731188
88. Yona S, Lin HH, Siu WO, Gordon S, Stacey M. Adhesion-GPCRs: emerging roles for novel receptors. *Trends Biochem Sci*. 2008; 33(10): 491–500. <https://doi.org/10.1016/j.tibs.2008.07.005> PMID: 18789697
89. Lee Y, Yoon KA, Joo J, Lee D, Bae K, Han JY, et al. Prognostic implications of genetic variants in advanced non-small cell lung cancer: a genome-wide association study. *Carcinogenesis*. 2013; 34(2): 307–13. <https://doi.org/10.1093/carcin/bgs356> PMID: 23144319
90. Russell T, Madsen T, Thomas F, Raven N, Hamede R, Ujvari B. Oncogenesis as a selective force: adaptive evolution in the face of a transmissible cancer. *Bioessays*. 2018; 40(3). <https://doi.org/10.1002/bies.201700146> PMID: 29446482
91. Wells K, Hamede RK, Kerlin DH, Storfer A, Hohenlohe PA, Jones M, et al. Infection of the fittest: devil facial tumour disease has greatest effect on individuals with highest reproductive output. *Ecol Lett*. 2017; 20(6): 770–778. <https://doi.org/10.1111/ele.12776> PMID: 28489304
92. Orsmond GI, Krauss MW, Seltzer MM. Peer relationships and social and recreational activities among adolescents and adults with autism. *J Autism Dev Disord*. 2004; 34(3): 245–56. PMID: 15264493
93. Walton KM, Ingersoll BR. Improving social skills in adolescents and adults with autism and severe to profound intellectual disability: A review of the literature. *J Autism Dev Disord*. 2013; 43(3): 594–615. <https://doi.org/10.1007/s10803-012-1601-1> PMID: 22790427
94. Taheri A, Perry A, Minnes P. Examining the social participation of children and adolescents with Intellectual Disabilities and Autism Spectrum Disorder in relation to peers. *J Intellect Disabil Res*. 2016; 60(5): 435–43. <https://doi.org/10.1111/jir.12289> PMID: 27120987
95. Hamede RK, Bashford J, McCallum H, Jones M. Contact networks in a wild Tasmanian devil (*Sarcophilus harrisii*) population: using social network analysis to reveal seasonal variability in social behaviour and its implications for transmission of devil facial tumour disease. *Ecol Lett*. 2009; 12(11): 1147–57. <https://doi.org/10.1111/j.1461-0248.2009.01370.x> PMID: 19694783
96. Catchen J, Hohenlohe PA, Bassham S, Amores A, Cresko WA. Stacks: an analysis tool set for population genomics. *Mol Ecol*. 2013; 22(11): 3124–40. <https://doi.org/10.1111/mec.12354> PMID: 23701397
97. Etter PD, Bassham S, Hohenlohe PA, Johnson EA, Cresko WA. SNP discovery and genotyping for evolutionary genetics using RAD sequencing. *Methods Mol Biol*. 2011; 772: 157–78. https://doi.org/10.1007/978-1-61779-228-1_9 PMID: 22065437
98. Purcell S, Neale B, Todd-Brown K, Thomas L, Ferreira MA, Bender D, et al. PLINK: a tool set for whole-genome association and population-based linkage analyses. *Am J Hum Genet*. 2007; 81(3): 559–75. <https://doi.org/10.1086/519795> PMID: 17701901
99. Benjamini Y, Hochberg Y. Controlling the false discovery rate: a practical and powerful approach to multiple testing. *Journal of the royal statistical society. Series B (Methodological)*. 1995; 57(1): 289–300.
100. Jorde PE, Ryman N. Unbiased estimator for genetic drift and effective population size. *Genetics*. 2007; 177(2): 927–35. <https://doi.org/10.1534/genetics.107.075481> PMID: 17720927
101. Murchison EP, Schulz-Trieglaff OB, Ning Z, Alexandrov LB, Bauer MJ, Fu B, et al. Genome sequencing and analysis of the Tasmanian devil and its transmissible cancer. *Cell*. 2012; 148(4): 780–91. <https://doi.org/10.1016/j.cell.2011.11.065> PMID: 22341448